A new time–temperature–transformation cure diagram for thermoset/thermoplastic blend: tetrafunctional epoxy/poly(ether sulfone)

Bong Sup Kim, Tsuneo Chiba and Takashi Inoue*
Department of Organic and Polymeric Materials, Tokyo Institute of Technology, Ookayama, Meguro-ku, Tokyo 152, Japan
(Received 3 September 1992)

For the cure process of a thermoset/thermoplastic blend, tetrafunctional epoxy resin/poly(ether sulfone)/dicyandiamide (100/25/5), we established a new time–temperature–transformation (TTT) cure diagram. The transformation here involves (1) onset of phase separation, (2) gelation, (3) fixation of the dimension of phase-separated structure, (4) end of phase separation and (5) vitrification. The onset and end of phase separation were characterized by the time variation of the invariant of light scattering (V_v) and the spatial fixation of phase-separated structure was by levelling off the decrease of scattering peak angle. The gelation and vitrification points were determined conventionally by rheological measurements, i.e. by a cross-over of dynamic storage modulus and dynamic loss modulus curves, and by torsional braid analysis curve, respectively. The epoxy/poly(ether sulfone) mixture was shown to exhibit lower critical solution temperature (*LCST*)-type phase behaviour (*LCST*=265°C). In the early stage of curing, the ternary system was at a single-phase regime. After an induction period, phase separation started by the spinodal decomposition mode, then the domain spacing increased with time, i.e. the structure grew self-similarly. When the system was gelled, the spacing simultaneously ceased to increase. Even after that, the invariant still continued to increase, implying further growth in concentration fluctuation. The invariant then levelled off and finally the whole system was vitrified by the increase in glass transition temperature of the epoxy-rich phase. This situation was described in terms of the new TTT cure diagram in wide ranges of cure temperature (130–250°C) and cure time (6 h).

(Keywords: blend; epoxy resin; poly(ether sulfone); light scattering; torsional braid analysis; d.s.c.; spinodal decomposition; TTT cure diagram)

INTRODUCTION

Curing of thermoset resin (e.g. epoxy resin) involves chain extension, branching and crosslinking. The chemical reaction usually causes a change in physical state, from a viscous liquid to a gel and then to a vitrified material. Gelation occurs due to crosslinking. Vitrification occurs due to the increase of the glass transition temperature (T_g), i.e. the system vitrifies when T_g reaches cure temperature. To characterize the change in physical state during curing, Gillham and Babayevsky[1] and Gillham[2] proposed the time–temperature–transformation (TTT) cure diagram on the basis of torsional braid analysis (TBA). The TTT cure diagram describes the transformations (gelation and vitrification) as functions of cure time and cure temperature.

In previous papers[3–5] we dealt with multicomponent thermoset resin systems, such as diglycidyl ether of bisphenol-A (epoxy)/poly(ether sulfone) (PES) and epoxy/liquid nitrile rubber systems. In the early stage of curing, the systems were at a single-phase regime. As the cure reaction proceeded, phase separation took place via the spinodal decomposition induced by the increase in molecular weight of the epoxy, resulting in a regularly separated two-phase structure. The unique structure was shown to be formed under a specific situation: competitive progress of phase separation and the crosslink reaction. Thus, the chemical reaction causes a complicated change in the physical state of the mixture, from a single-phase liquid to the phase-separated liquid and eventually to a phase-separated, crosslinked and vitrified material. Hence, to characterize the cure process of a multicomponent thermoset resin system, one has to describe the structure development in terms of (1) onset of phase separation, (2) gelation, (3) fixation of the phase-separated structure, (4) end of phase separation and (5) vitrification.

In this paper we deal with a tetrafunctional epoxy/PES blend and investigate the reaction kinetics by d.s.c., the phase-separation process by light scattering, and the gelation and vitrification processes by viscoelastic measurements, to establish a new TTT cure diagram. The new diagram describes the five stages of transformation cited above.

EXPERIMENTAL

A tetrafunctional epoxy resin, tetraglycidyl 4,4′-diamine-diphenylmethane, was supplied by Yuka-Shell Epoxy Co.

* To whom correspondence should be addressed

0032-3861/93/132809-07

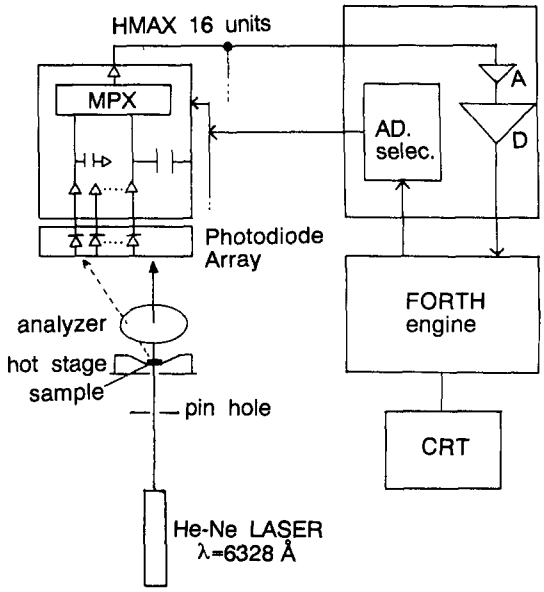

Figure 1 Light scattering apparatus

(Epikote 604). The curing agent was dicyandiamide (DICY). Poly(ether sulfone) (PES) was supplied by Mitsui Toatsu Co. (ICI Victrex 4100P; $M_n = 17.7 \times 10^3$).

The epoxy and PES were dissolved at 10 wt% of total polymer in methylene chloride. The solution was cast onto a cover glass (for microscopy). The cast film was further dried under a vacuum of 10^{-4} mmHg for 12 h. The film on the cover glass was inserted in a heating stage (Linkam TH 600 heating–cooling stage) programmed to provide a linear rise in temperature at two different rates: 5 and 10°C min^{-1}. During the linear temperature rise, we observed the onset of phase separation under the light microscope. Based on this observation, we obtained the phase diagram of the epoxy/PES mixture.

We also prepared solution-cast film of the mixture loaded with DICY in the same way. The ternary mixture (epoxy/PES/DICY) on the cover glass was annealed in the hot chamber set horizontally on the light scattering stage, as shown in *Figure 1*. Radiation of wavelength 632.8 nm from a He–Ne gas laser was applied vertically to the film. The intensity of scattered light from the film was measured under an optical alignment with parallel polarization. The angular distribution of scattered light intensity was detected by a one-dimensional photometer with a 46 photodiode array (HASC Co. Ltd). The scattering profiles in a time of 1/30 s were recorded at appropriate intervals during isothermal annealing (curing) and were stored in a Forth Engyne computer for further analysis. A light scattering pattern was also observed by using a photographic technique similar to that of Stein and Rhodes[6].

SEM observation was carried out in three ways: (1) conventional secondary electron image (SEI) for fractured surface; (2) SEI for fractured and etched surface; and (3) compositional image (CI) by the backscattered electrons from a microtomed (flat) surface[7]. Here the specimen was fractured at liquid nitrogen temperature. Etching was carried out by immersing the fractured specimen in methylene chloride at room temperature for 24 h, and the microtoming was by ultramicrotome (Ultracut N, Reichert-Nissei) equipped with cryostat (FA 4E, Reichert-Nissei).

The cure reaction kinetics was followed by d.s.c. (Du Pont, model 910). The conversions (degree of reaction) of neat epoxy and the epoxy/PES mixtures were estimated by the area of the exotherm peak (temperature range 100–350°C) evolving from the reaction during the d.s.c. heating run at 10°C min^{-1}. That is, the conversion was given by:

$$\text{Conversion} = \left(1 - \frac{A_t}{A_0}\right) \times 100\%$$

where A_0 is the area of the exotherm peak of uncured material and A_t is that of cured material.

The gel point was estimated by the viscoelastic analysis proposed by Chambon and Winter[8,9] as a cross-over point of the dynamic storage modulus G' and the dynamic loss modulus G'' curves*. G' and G'' were measured by a Rheometrics Dynamic Spectrometer (model RDS-7700) fitted with parallel-plate test cell (plate radius 12.5 mm, gap 1.0 mm) as a function of cure time at various temperatures.

To analyse the vitrification at late stages of curing, the changes in the relative modulus and the damping with curing were measured by TBA using a Rheolograph TBA (model 562, Toyo Seiki Co.). The vitrification point was determined as described later.

RESULTS AND DISCUSSION

Phase diagram of epoxy/PES mixture

The solution-cast film of the binary mixture of epoxy and PES was transparent and homogeneous under the light microscope. During the linear temperature rise in the binary mixture, the onset of phase separation was observed under the light microscope when the temperature reached a certain value, T_s (T_s is shown by circles in *Figure 2*). Plotting T_s *versus* heating rate, we obtained an intercept of T_s at which the heating rate is zero. The intercept temperature may correspond to the binodal temperature (the binodal points thus estimated are shown by triangles in *Figure 2*), indicating lower critical solution temperature (*LCST*)-type phase behaviour. *Figure 2* also shows the T_g curve, estimated by the Fox equation using the d.s.c. data of epoxy and PES.

On the basis of current understanding of polymer–polymer miscibility, the *LCST* in *Figure 2* is expected to decrease, and the two-phase regime would prevail in the phase diagram as the molecular weight of epoxy increases with curing. The T_g of the mixture would be elevated when the molecular weight increases. These situations are demonstrated schematically in *Figure 2*. *Figure 2* implies that the mixture of composition ϕ is initially at a single-phase regime at T_{cure}; however, the system will be thrust into a two-phase regime as the curing reaction proceeds. Hence, the spinodal decomposition is expected to take place in the curing process.

Cure reaction kinetics

Figure 3 shows typical d.s.c. thermograms of an uncured and a partially cured blend. Here a ternary system, epoxy/PES/DICY (100/25/5) was cured at 190°C

* Before gelation, the viscous character prevails over the elastic one ($G' > G''$), while the latter dominates after gelation ($G' < G''$) and $G' = G''$ at the gel point

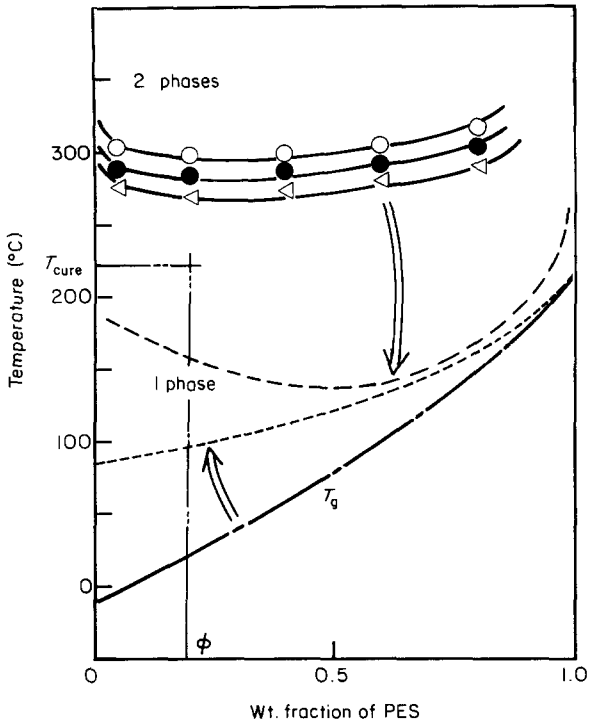

Figure 2 Phase diagram of tetrafunctional epoxy/PES mixture. Heating rate: ○, 10°C min^{-1}; ●, 5°C min^{-1}; ▽, zero (extrapolated)

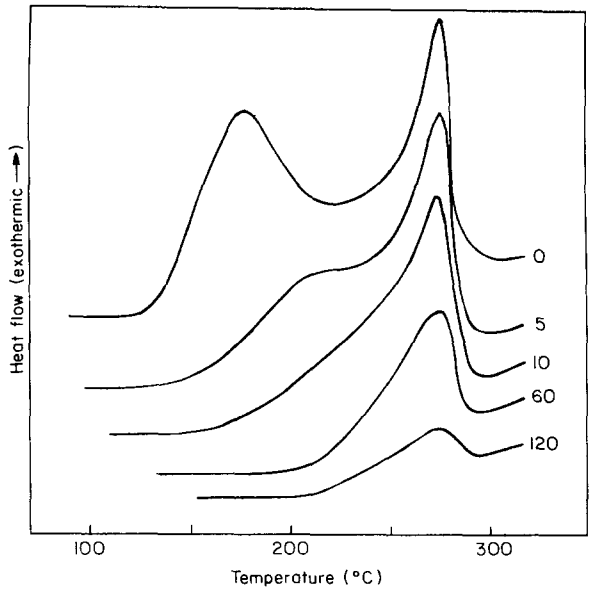

Figure 3 D.s.c. thermograms of uncured and partially cured blend: tetrafunctional epoxy/PES/DICY (100/25/5) cured at 190°C. Cure time (min) is given next to each curve

(for different times) and was then subjected to d.s.c. measurement. As shown in the figure, after curing for a short time the system exhibits two exotherm peaks. The first peak may be related to a reaction of primary amine and the second to that of secondary amine. The longer the cure time, the smaller is the peak area. The conversion estimated by the peak area in *Figure 3* is plotted as a function of the cure time in *Figure 4*. The reaction in the blend is slower than that in the neat epoxy system. The delay may be caused by reduced mobility due to the loading of high T_g component (PES) so that it becomes more significant at lower temperatures.

Structure development by light scattering and SEM

An epoxy/PES mixture loaded with DICY (epoxy/PES/DICY = 100/25/5) was also a single-phase system at the curing temperature and no appreciable light scattering was detected from the mixture in the early stages of curing. After an induction period, a ring pattern of light scattering appeared, as shown in *Figure 5*. The ring pattern implies the development of regularly phase-separated structure. The ring pattern became brighter and its diameter decreased with curing time. This situation is demonstrated by the change in the light scattering profile with cure time in *Figure 6*. The ring pattern and the characteristic change in scattering profile are the hallmarks of spinodal decomposition.

One can estimate the periodic distance, Λ_m, in the phase-separated structure as a Bragg spacing from the peak angle, θ_m, of the scattering profile in *Figure 6*:

$$\Lambda_m = \lambda(2 \sin \theta_m)^{-1}$$

where λ is the wavelength of light in the medium. The variation of Λ_m with cure time is shown in *Figure 7*. Λ_m increases with time and eventually levels off, suggesting

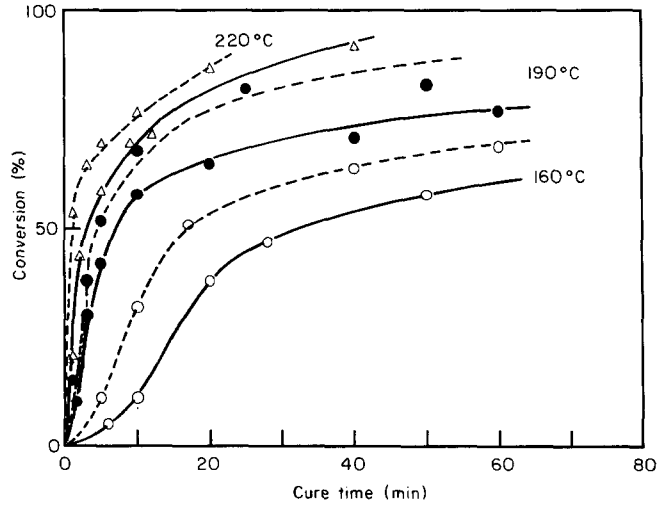

Figure 4 Time–conversion curves at various cure temperatures. ---, Epoxy/DICY (100/5); ——, epoxy/PES/DICY (100/25/5)

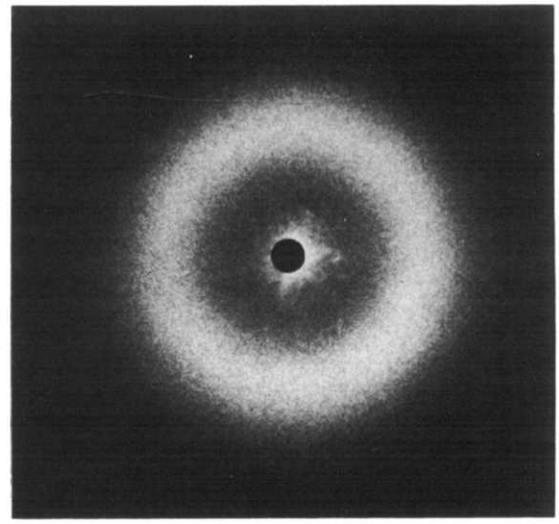

Figure 5 Light scattering pattern. The scattering profile of this ring pattern is shown in *Figure 6* (curve for 2000 s)

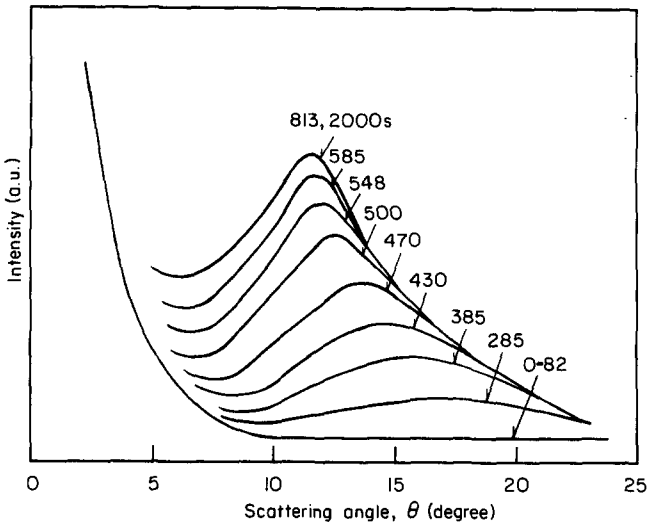

Figure 6 Change in the light scattering profile with curing: tetrafunctional epoxy/PES/DICY (100/25/5) cured at 190°C. The numbers shown are the cure times

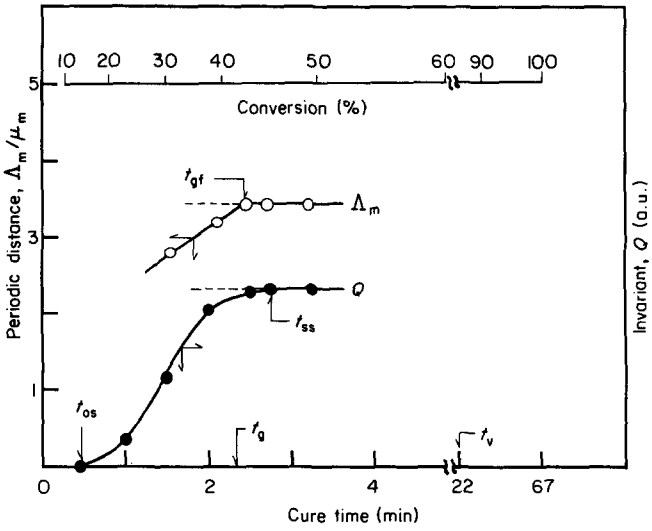

Figure 7 Time variation of periodic distance Λ_m and invariant Q during curing; tetrafunctional epoxy/PES/DICY (100/25/5) at 220°C

that further growth of the structure is suppressed by gelation (as will be discussed later). We denote the levelling off point as the time of geometry fixation, t_{gf}.

Figure 8 shows scanning electron micrographs of cured resin. The micrographs are the composition images using backscattered electrons from a flat-microtomed surface. The dark region is ascribed to the epoxy-rich phase with a lower atomic number, while the bright region corresponds to the PES-rich phase (see Appendix). Epoxy-rich globules with uniform diameter of a few micrometres are dispersed in a PES-rich matrix. Note that the periodic distances between the globules in SEM exactly correspond to those obtained by light scattering in *Figure 7*.

It is hard to discuss the onset of phase separation from the time variation of the scattering profile itself. To discuss the onset, it is convenient to employ the integrated scattering intensity, i.e. the invariant Q defined by

$$Q = \int_0^\infty I(q) q^2 \, dq$$

where q is the scattering vector, $q = (4\pi/\lambda) \sin\theta$, and $I(q)$ is the intensity of the scattered light at q. Since the invariant Q from an optically isotropic system with concentration fluctuation is ascribed to the mean-square concentration fluctuation[10], it is a more appropriate and more sensitive quantity for the degree of phase separation than the profile itself. The Q values are plotted in *Figure 7*. From the plot one can determine the onset time of phase separation, t_{os}, and also the time at which phase separation ends t_{ss}. As shown in the figure, t_{ss} is larger than t_{gf}, i.e. even after the geometry fixation, phase separation proceeds further, suggesting a further increase in the composition difference between PES-rich and epoxy-rich regions. *Figure 7* also shows the time–conversion scale, the gelation time t_g and

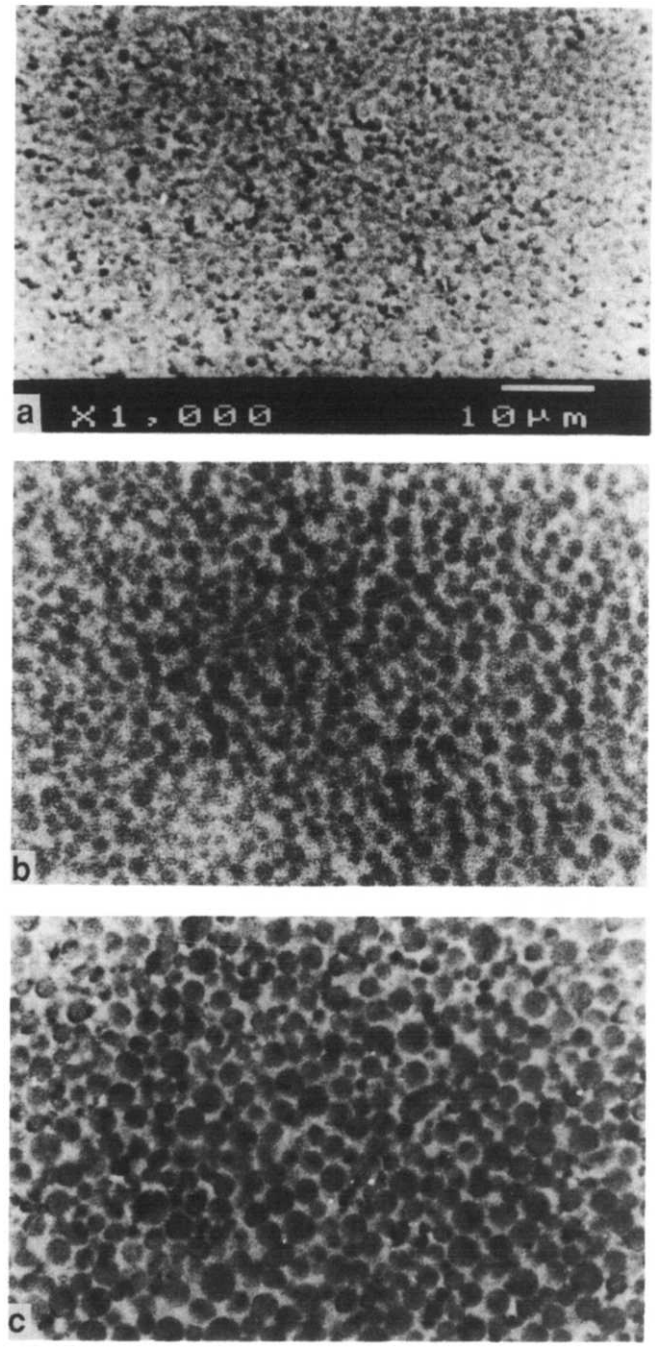

Figure 8 SEM (composition image by backscattering) of tetrafunctional epoxy/PES/DICY (100/25/5) cured at 190°C. Cure time (min): (a) 2; (b) 6; (c) 30

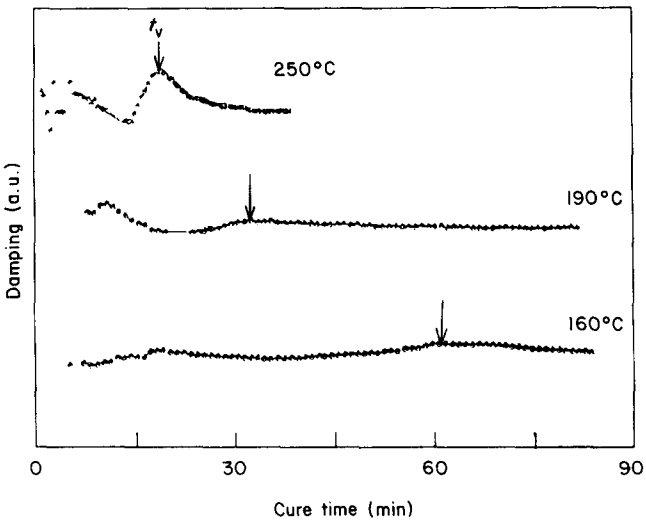

Figure 9 TBA damping curves of tetrafunctional epoxy/PES/DICY (100/25/5) at various cure temperatures

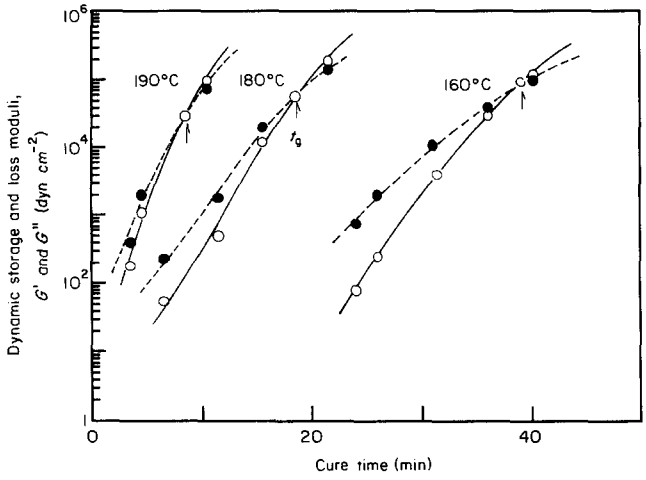

Figure 10 Time variation of dynamic storage modulus G' (○) and dynamic loss modulus G'' (●) at various cure temperatures, at 1.6 Hz

the vitrification time t_v (by viscoelastic measurements, see below) for reference.

Gelation and vitrification

Figure 9 shows TBA damping curves of epoxy/PES/DICY (100/25/5) at three isothermal settings. The first damping peak is ascribed to the gel point and the second to the vitrification point[1]. However, at high temperature (e.g. 250°C) the first peak is not obvious and it is hard to determine the gel point. Normal operation of the TBA instrument cannot be achieved due to the fast reaction, which provides a short time for the onset of gelation. Consequently, we switched from the TBA method to the Rheometrics analysis for

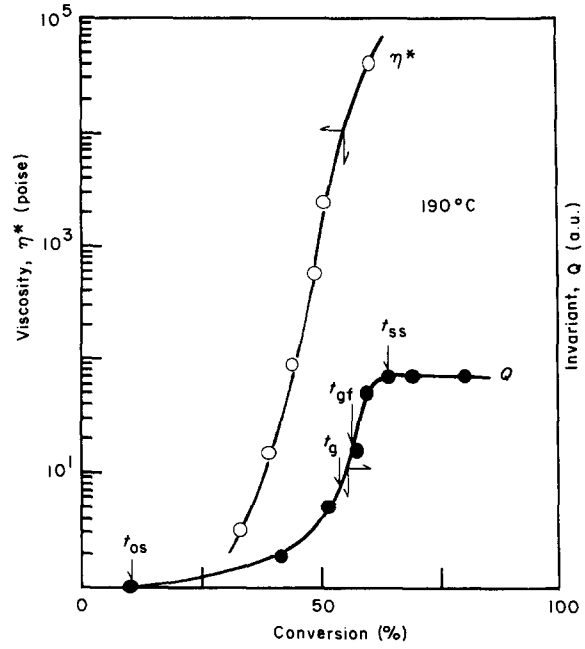

Figure 11 Complex viscosity η^* (○) and invariant Q (●) as a function of conversion

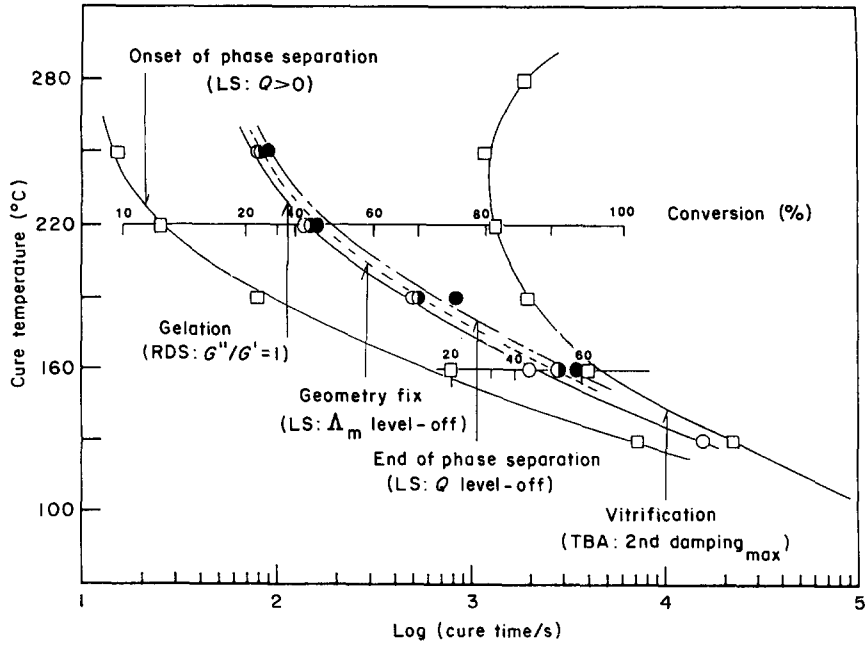

Figure 12 A new TTT cure diagram (LS, light scattering; RDS, Rheometrics dynamic spectrometer; TBA, torsional braid analysis)

the gel point measurement. However, the vitrification point was determined by TBA and a time at the second TBA peak is denoted as the vitrification time t_v. The results are shown in *Figure 12*.

Figure 10 shows the variations of the dynamic storage modulus G' and the dynamic loss modulus G'' with cure time at three cure temperatures. At early stages of curing, G'' is much higher than G'. At later stages G' becomes higher than G''. Following the proposal by Chambon and Winter[8,9] the cross-over point of $G'(t)$ and $G''(t)$ curves was assumed to be the gel point. Thus, we defined the gelation time t_g. The results are summarized in *Figure 12*.

From the viscoelastic measurement, one can also calculate the complex viscosity η^*:

$$\eta^* = (G'^2 + G''^2)^{1/2}/\omega$$

where ω is the oscillating frequency. The calculated results are plotted as a function of conversion in *Figure 11*, where light scattering invariant Q is also plotted. Phase separation starts in the liquid state with very low viscosity and gelation takes place at a viscosity of the order of 10^4 poise. A dramatic change in viscosity (four decades) is seen with cure reaction.

A new TTT cure diagram

Summarizing the results of light scattering, TBA, dynamic viscoelastic analysis and d.s.c., one can establish a new TTT cure diagram as shown in *Figure 12*. Here, on the conventional TTT cure diagram associated with gelation and vitrification, other transformations characteristic of the multicomponent thermoset system are described in terms of the onset of phase separation, the fixation of the dimension of phase-separated structure and the end of phase separation. The new TTT cure diagram shows that the system is initially at a single-phase regime, phase separation starts after an induction period, gelation and structure fixation take place almost simultaneously, the end of phase separation follows, and finally the system is vitrified, in a wide cure temperature range. Note that such transitions take place in various time scales, depending on the temperature.

REFERENCES

1 Gillham, J. K. and Babayevsky, P. G. *J. Appl. Polym. Sci.* 1973, **17**, 2067
2 Gillham, J. K. 'Development in Polymer Characterization-3' (Ed. J. V. Dawkins), Applied Science Publishers, London, 1982, Ch. 5
3 Yamanaka, K. and Inoue, T. *Polymer* 1989, **30**, 662
4 Yamanaka, K., Takagi, Y. and Inoue, T. *Polymer* 1989, **30**, 1839
5 Yamanaka, K. and Inoue, T. *J. Mater. Sci.* 1990, **25**, 241
6 Stein, R. S. and Rhodes, M. B. *J. Appl. Phys.* 1969, **31**, 1873
7 Goizueta, G., Chiba, T. and Inoue, T. *Polymer* 1992, **33**, 674
8 Chambon, F. and Winter, H. H. *Polym. Bull.* 1985, **13**, 499
9 Chambon, F. and Winter, H. H. *J. Rheol.* 1986, **30**, 367
10 Koberstein, J., Russel, T. P. and Stein, R. S. *J. Polym. Sci., Polym. Phys. Edn* 1979, **17**, 1719
11 Kim, B. S., Chiba, T. and Inoue, T. to be published

APPENDIX: COMPOSITION IMAGE BY SEM

Two-phase structure in polymer blends is often investigated by SEM. Usually a micrograph is obtained by collecting secondary electrons from a fractured surface. This secondary electron image (SEI) gives information about the topology of the fractured surface. When adhesion between the phases is poor, SEI successfully reveals the two-phase structure. However, in the case of strong adhesion, SEI might be just a fractographic view which is far from the two-phase structure itself. To avoid such artefacts, the selective etching method is employed; this involves immersing the fractured specimen in a selective solvent, and rinsing to remove the soluble component, thus revealing the holes which are visualized by SEI SEM. We recently proposed another SEM technique: SEM observation of a microtomed and stained specimen using backscattered electrons[7]. That is, the stained specimen is microtomed to provide a flat surface, the microtomed specimen is stained (e.g. by

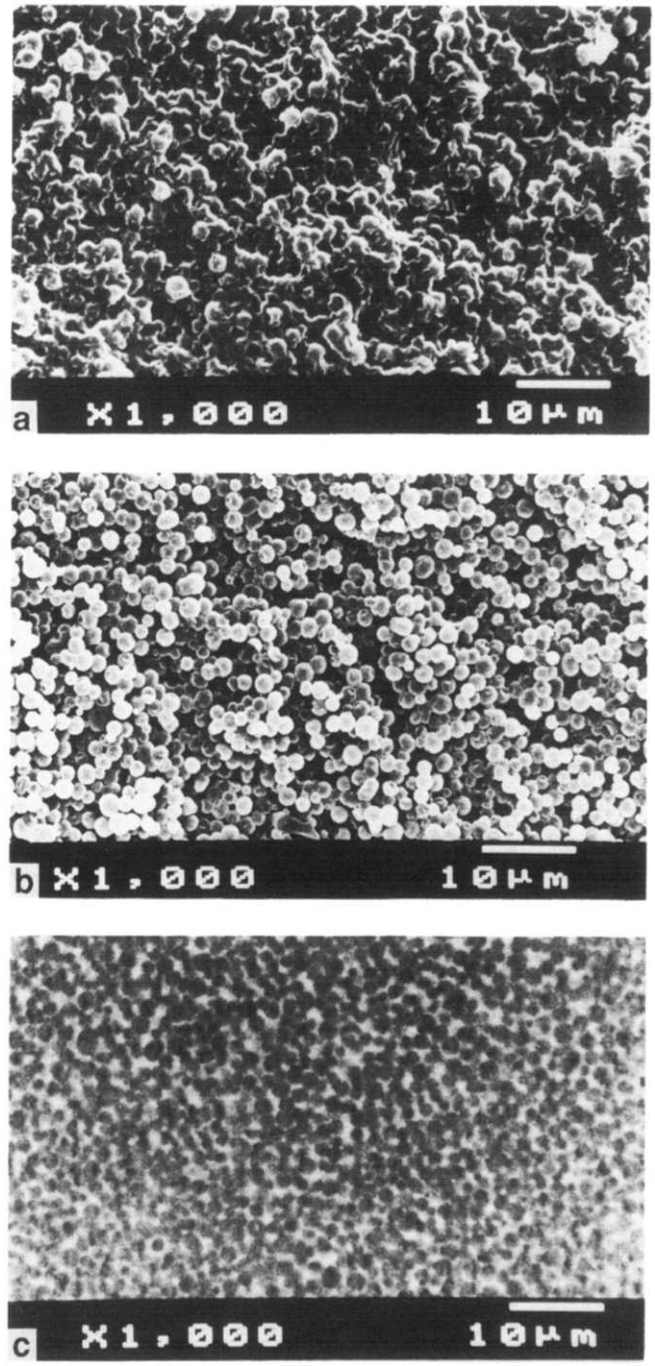

Figure 13 SEM micrographs, of tetrafunctional epoxy/PES/DICY (100/25/5) cured at 160°C for 24 h, obtained by three different methods: (a) fractured (secondary electron image); (b) fractured and etched (secondary electron image); (c) microtomed (composition image)

OsO_4) and the composition image (CI) is obtained by collecting backscattered electrons.

Figure 13 shows SEM results for a cured epoxy/PES/DICY system by the three methods mentioned above. SEI of a fractured surface (*Figure 13a*) seems to provide less information on the two-phase structure than the other two methods (*Figures 13b* and *c*), but it may be helpful in understanding the fracture mechanism of the two-phase material.

In the SEI of a fractured and etched surface (*Figure 13b*), PES is assumed to be rinsed away and the remaining material is a crosslinked epoxy. Fine globules with uniform diameter are arranged quite regularly and seem to be connected to each other. This connectivity could be interpreted by the structure formation mechanism via the spinodal decomposition, as discussed in the previous paper[3].

The Cl of a microtomed surface (*Figure 13c*) supports the phase assignment in *Figure 13b*, i.e. epoxy globules in PES matrix, since a phase having higher atomic number (PES) should be the bright area of CI. Unfortunately, the CI SEM does not reveal the three-dimensional view so that the connectivity of globules is not obvious in *Figure 13c*. However, the CI method would be powerful for an unetchable system such as thermoset/thermoset and thermoset/reactive-thermoplastic blends[11]. Note that the CI in *Figure 13c* is from the unstained surface. This suggests that staining is not necessary for this particular blend.